Available online at www.sciencedirect.com
ScienceDirect
Estuarine, Coastal and Shelf Science 78 (2008) 14–26
ESTUARINE COASTAL AND SHELF SCIENCE
www.elsevier.com/locate/ecss

Diatom succession and silicon removal from freshwater in estuarine mixing zones: From experiment to modelling

Vincent Roubeix*, Véronique Rousseau, Christiane Lancelot

Université Libre de Bruxelles, Ecologie des Systèmes Aquatiques (ESA), CP-221, Boulevard du Triomphe, B-1050 Bruxelles, Belgium

Received 30 May 2007; accepted 13 November 2007
Available online 19 November 2007

Abstract

Estuaries act as filters for land derived material reducing the river input to the coastal zone. Silicon (Si) removal from freshwater which is tightly linked to the growth of diatoms was studied in the estuarine mixing zone where the mixing of freshwater and seawater results in a salinity gradient. Three planktonic diatom species with different origin and salinity tolerance were grown in an artificial salinity gradient. Salinity stress and nutrient depletion led to a specific succession of the three diatoms along the salinity gradient. When available light was increased, diatoms reached higher biomass and the Si removal from water column was more efficient along the mixing. From this experiment, a conceptual model of Si transformations and removal from freshwater was build and applied to an idealized stratified estuary. Sensitivity analysis with varying initial conditions and parameter values pointed transit time of freshwater in the estuary, freshwater and seawater mixing rate and river turbidity as important interactive factors influencing Si removal from freshwater. Other factors like the total amount and the salinity tolerance of diatoms in the upstream river were shown to significantly affect riverine Si removal from the surface layer of an estuary. Finally it appears that Si removal from freshwater in estuarine mixing zones proceeds in two ways: a first rapid death and sedimentation of planktonic stenohaline diatoms imported from the river and second, the growth and subsequent settling of planktonic euryhaline diatoms of either freshwater or marine origin.
© 2007 Elsevier Ltd. All rights reserved.

Keywords: diatoms; salinity gradients; ecological succession; silica; estuaries

1. Introduction

Diatoms have an absolute requirement for silicic acid (DSi), a dissolved source of silicon (Si) whose shortage in the water column can limit their growth. Depletion of DSi relative to inorganic nitrogen and phosphate has been shown to select for non-siliceous algae (Smayda, 1990; Egge and Aksnes, 1992). As conceptually discussed in Officer and Ryther (1980) and Billen et al. (1991), this shift is exacerbated in coastal waters receiving anthropogenic inputs of nitrogen and phosphorus and can result in the dominance of often poorly edible non-siliceous algae, with undesirable trophic and environmental consequences. A well known example of such change in dominance of the phytoplankton community are the recurrent *Phaeocystis* colony blooms in the Southern Bight of the North sea (Lancelot and Mathot, 1987).

Before reaching the coastal sea, riverine Si passes through estuaries which act as filters for land derived material (Billen et al., 1991; Dettmann, 2001; Humborg et al., 2003). According to the definition of Pritchard (1967), ''an estuary is a semi-enclosed coastal body which has a free connection with the open sea and within which seawater is measurably diluted with freshwater derived from land drainage''. The salinity gradient resulting from the mixing of freshwater and seawater is one specific hydrological aspect of estuaries which is not found in other filter systems in the land-ocean continuum (Billen et al., 1991). The estuarine mixing zone is the part of the estuary where a seaward gradual increase of salinity takes place. Its upper limit of salinity depends on the physical downstream boundary given to the estuary and on the mixing conditions in the estuary.

* Corresponding author.
E-mail address: vroubeix@ulb.ac.be (V. Roubeix).

0272-7714/$ - see front matter © 2007 Elsevier Ltd. All rights reserved.
doi:10.1016/j.ecss.2007.11.007

Fast decay of freshwater phytoplankton including diatoms has often been reported in estuaries (Morris et al., 1978; Ahel et al., 1996; Muylaert and Sabbe, 1999; Ragueneau et al., 2002). This mortality occurs generally at low salinity (0–10) and is attributed to osmotic stress on freshwater phytoplankton cells as salinity increases. However, some phytoplankton species are less affected by salinity change and grow along the salinity gradient provided that light and nutrients are sufficient (Orive et al., 1998). These two controlling factors of phytoplankton growth have generally opposite evolution along the salinity gradient because of the gradual mixing of the nutrient-rich but turbid river water with the clearer and nutrient-poorer seawater as observed by DeMaster et al. (1996) in the Amazon and by Humborg (1997) in the Danube.

Riverine Si is transported as DSi, particulate biogenic ($bSiO_2$) or lithogenic silica. The transformations of Si are mainly driven by the growth of diatoms controlling the uptake of DSi and its precipitation into $bSiO_2$ and by the dissolution of dead diatom frustules ($bSiO_2$) releasing DSi. Si removal from freshwater in an estuarine mixing zone implies the sedimentation of riverine silica out of a mixed brackish layer which has a seawards residual flow. Removed Si from freshwater is retained at more or less long term in the deep estuary (marine layer) or in the sediments. It can be then re-injected into the mixed brackish layer after silica dissolution followed by diffusion, entrainment or mixing, or it can be permanently stored and preserved in the sediments after its burial or remineralisation. Whatever is the fate of settled riverine Si, its removal from freshwater either delays or decreases the Si delivery to the coastal zone and might exacerbate Si limitation especially in a context of anthropogenic eutrophication where nitrogen and phosphorus are generally in excess.

In this study, we investigated Si transformations and removal in estuarine mixing zones by conducting a freshwater and seawater mixing experiment with different diatom species and by sensitivity analysis with a conceptual model applied to an idealized estuary. Previous experiments have already explored the chemical and biological mechanisms of Si transformations in reconstructed estuarine mixing zones. Bien et al. (1958) showed indeed DSi removal by mixing freshwater from the Mississippi River with seawater from the Gulf of Mexico. The observed DSi depletion was attributed to diatom uptake and adsorption on suspended organic matter. However, later studies reported a marginal abiotic uptake of DSi in estuaries (Chou and Wollast, 2006) while diatom uptake is by far the dominant process. Lionard et al. (2005) showed that a salinity shift from 0.5 to 10 clearly affected the growth of chlorophytes and diatoms, partially explaining the replacement of freshwater species by marine species generally observed in the Schelde estuary in this salinity range. In the same way, Ragueneau et al. (2002), by mixing water from the Danube river with filtered water from the Black Sea gave evidence of freshwater diatom mortality at low salinity (<5). As a further step, we here carried out the progressive mixing of an artificial freshwater medium with filtered water from the Southern Bight of the North Sea in the presence of three planktonic diatom species isolated at different levels of the river-sea continuum. These are *Asterionella formosa* Hass, chosen as typically freshwater diatom, *Cyclotella meneghiniana* Kützing, a widespread euryhaline freshwater-brackish diatom (Finlay et al., 2002) and *Skeletonema costatum* Cleve, a common coastal diatom. The mixing experiment was conducted at two different levels of irradiance to assess the added effect of light availability on Si transformations and removal along the mixing. From this experiment, a conceptual mechanistic model was built accounting for the main transformations of Si during river and seawater mixing in an idealized stratified estuary and sensitivity analysis was performed to identify the driving forces behind Si removal from freshwater in estuarine mixing zones.

2. Materials and methods

2.1. Diatom cultures

Asterionella formosa was isolated from Cumbrian lakes (Culture Collection of Algae and Protozoa, N° 1005/9), *Cyclotella meneghiniana* from the freshwater reaches of the Schelde estuary and *Skeletonema costatum* from the Belgian coastal zone. The three species were maintained in separated culture flasks in a growth cabinet at 20 °C illuminated with a 14:10 light-dark cycle at 100 µmol quanta m^{-2} s^{-1}. *Skeletonema costatum* was grown in f2 medium (Veldhuis and Admiraal, 1987) composed of seawater in which major nutrients, trace and minor elements and vitamins are added. For *A. formosa* and *C. meneghiniana*, the WH culture medium prepared with milli-Q water was used (Guillard and Lorenzen, 1972) which is the freshwater equivalent of the f2 medium.

2.2. Experiments

2.2.1. Diatom batch cultures at constant salinity

The effect of salinity on the growth rate of the three diatom species was investigated by incubating the different pure cultures at salinities 0, 2, 5, 10, 18, 25, 30 and 33, at 20 °C and under optimal nutrient and light conditions (continuous light; 130 µmol quanta m^{-2} s^{-1}). The different salinity media were obtained by dilution of artificial seawater (Harrison et al., 1980) with milli-Q water while nutrient conditions were those of the WH medium for *Cyclotella meneghiniana* and *Asterionella formosa* and f2 for *Skeletonema costatum*. After a first growth phase of adaptation to the new salinity, the cultures were diluted with fresh medium and growth rates were determined spectrophotometrically based on the evolution of the optical density at 750 nm (Sorokin, 1973; Shafik et al., 1997). For *A. formosa* the optical density was not correlated to the actual cell number probably because of its colonial form. Growth rate of *A. formosa* was then estimated from direct cell counts (see Section 2.3). Growth rate μ was estimated by fitting of the exponential growth equation:

$$\mu = \frac{\ln X(t_2) - \ln X(t_1)}{(t_2 - t_1)}$$

Where X is a biomass index (optical density or cell number) and $(t_2 - t_1)$ is a time interval in the exponential growth phase.

2.2.2. Gradual mixing of freshwater and seawater diatom cultures

Estuarine diatom dynamics and Si transformations were investigated by the mixing of freshwater and seawater at a temperature of 20 °C after the experimental design of Fig. 1. A continuous culture of *Skeletonema costatum* (*c*) was progressively mixed with two bi-specific freshwater cultures of *Asterionella formosa* and *Cyclotella meneghiniana* growing at high (*a*) and low (*b*) light.

A mixed culture of *Asterionella formosa* and *Cyclotella meneghiniana* was prepared in WH medium and divided into flasks *a* and *b* (Fig. 1). The continuous culture of *Skeletonema costatum* (*c*) received a constant inflow from flask *d* at a rate of 0.4 d^{-1} and had reached equilibrium before the experiment started. Flask *d* contained 0.2 µm filtered, autoclaved seawater collected in the Southern Bight of the North Sea (Belgian coastal waters) at salinity 33 and enriched with f2 medium for a final DSi concentration of 7 µmol L^{-1}. Cultures *a* and *c* were grown under a continuous irradiance of 60 µmol quanta m^{-2} s^{-1} while a lower irradiance of 30 µmol quanta m^{-2} s^{-1} was imposed to culture *b* using a grey neutral density filter. Air bubbling was adjusted at a moderate intensity in each flask to mix the cultures and maintain living cells in suspension without preventing sedimentation of diatom detritus. An outflow was adapted so that the volume of each bottle remained constant.

During the experiment, cultures *a* and *b* were diluted with culture *c* at a rate of 0.09 d^{-1} to reach a salinity of 28 after 20 days when the mixing was stopped. Some 100 mL water samples were daily taken from cultures *a* and *b* for diatom cell and frustule counting and DSi and salinity measurements.

2.3. Measurements

Salinity was determined using a conductimeter (Cyberscan, Eutech instruments) and a salinity-to-conductivity relationship established from the dilution of the collected seawater of salinity 33.

For $bSiO_2$ and DSi determination, 50 mL samples were filtered on 47 mm diameter polycarbonate membrane Nucleopore filters (0.6 µm pore size). The $bSiO_2$ collected on filters was incubated for digestion in 0.1 M NaOH at 100 °C during 1 h and then neutralized with 1N HCl (Paasche, 1980a). The product of digestion (former $bSiO_2$) and the filtrate (DSi) were analyzed spectrophotometrically with the silicomolybdate method (Grasshoff et al., 1983). Prior to DSi determination, multiple calibrations at different salinities were carried out to establish a correction factor accounting for the effect of salinity on sample coloration.

The cell density (in cell L^{-1}) of each diatom species was estimated by cell counting under inverted microscopy (Leitz, Fluovert). Empty frustules were also enumerated in order to estimate the total concentration of frustules of each species (i.e. cells + empty frustules).

3. Results

3.1. Experiments

3.1.1. Diatom growth rates at constant salinity

Fig. 2 compares the salinity tolerance of *Asterionella formosa*, *Cyclotella meneghiniana* and *Skeletonema costatum* expressed in % of the specific maximal growth rate at various salinities from 0 to 33. The three diatom species differed clearly by their optimal salinity for growth which was 0, 18 and 33 for *A. formosa*, *C. meneghiniana* and *S. costatum* respectively. The growth rate of *A. formosa* was much affected by salinity with a 40% drop between salinity 0 and 2 and no growth observed at salinities higher than 2 (Fig. 2). Salinity 2 seems to be an absolute threshold as no growth was observed in a supplementary test after transferring the growing culture from salinity 2 to 5 in order to expose the cells to a more progressive salinity change. *Cyclotella meneghiniana* showed on the contrary a good tolerance to salinity with an optimal growth rate at intermediate salinity between river and sea

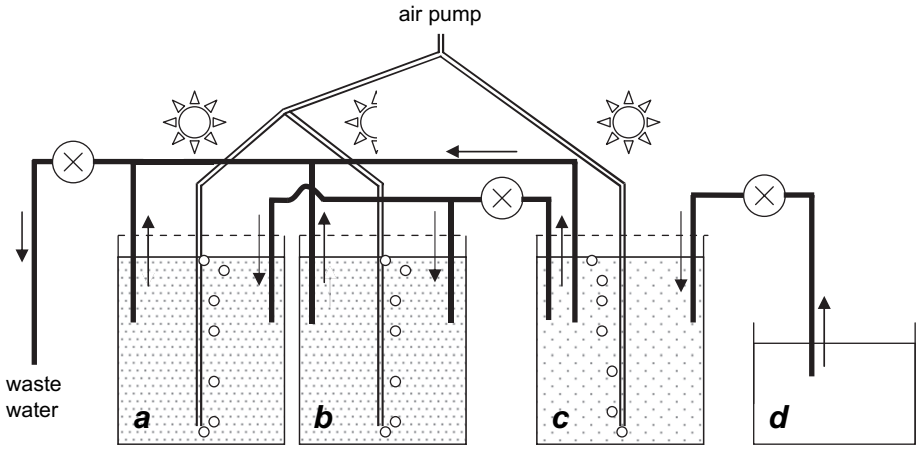

Fig. 1. Experimental design of freshwater and seawater mixing. The 4 flasks initially contained (from left to right) nutrient-enriched freshwater with 2 diatoms (*A. formosa* and *C. meneghiniana*) at high (*a*) and low (*b*) light, a continuous culture of a coastal diatom (*S. costatum*) (*c*) and nutrient-enriched filtered seawater (*d*). Arrows show the direction of water transport by the peristaltic pump (circled crosses) during mixing.

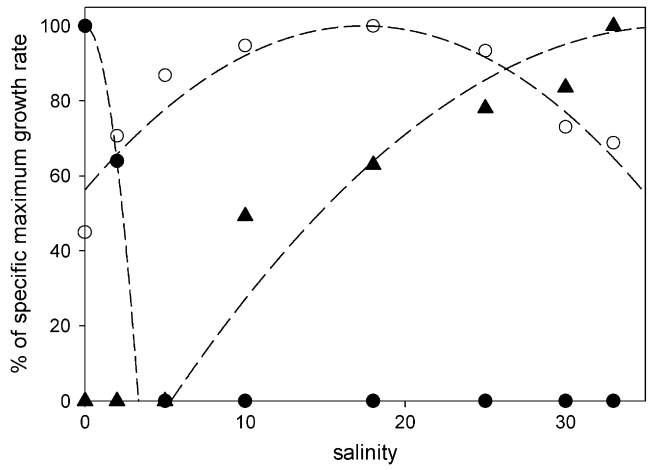

Fig. 2. Changes in relative growth rate of the diatoms *A. formosa* (●), *C. meneghiniana* (○) and *S. costatum* (▲) when inoculated from their maintenance culture medium into diluted artificial seawater at different salinities. The dashed lines represent the computed net growth rate of the three diatoms using a specific salinity-dependant mortality function (see Section 3.2.1).

(Fig. 2). However, its maximal growth rate was reduced by about 50% at salinity 0 and 33 showing a parabolic salinity-tolerance curve. *Skeletonema costatum* was not able to grow at salinities <10. At salinity 10, its growth rate was half of its maximum at salinity 33 suggesting a sharp change in salinity tolerance between 5 and 10 and a slight increase from 10 to 33.

3.1.2. Diatom dynamics and Si removal in an artificial salinity gradient

The obtained salinity curves show that the mixing of seawater with freshwater was regular along the experiment and identical at low and high light (Fig. 3). The artificial salinity gradient generated a succession of the three diatom species with a successive dominance of *Asterionella formosa*, *Cyclotella meneghiniana* and *Skeletonema costatum* independently on the imposed light level. Under high light (Fig. 3a), the salinity increase at the beginning of the gradient led to the immediate decrease of *A. formosa* abundance which reached a minimum on day 4. However, *A. formosa* showed a moderate peak on day 7 when salinity was about 15. This contrasts with the previous experiment which suggested that this diatom was unable to grow at salinity ≥5 (Fig. 2). After day 10, *A. formosa* completely disappeared from the water column (Fig. 3a). *Cyclotella meneghiniana* started exponential growth at salinity 5, reaching its maximal abundance on day 5 (salinity 12). After day 5, *C. meneghiniana* decreased up to its initial abundance on day 15 and remained at that level during the five next days. *Skeletonema costatum* did not appear until day 15 (salinity 25) when it started to grow exponentially till the end of the experiment.

The same trends were observed in the evolution of the abundance of each species along the salinity gradient under lower light (Fig. 3b). However, the lower light availability led generally to lower abundance maxima reached by each species, a delayed peak of *Cyclotella meneghiniana* and a later

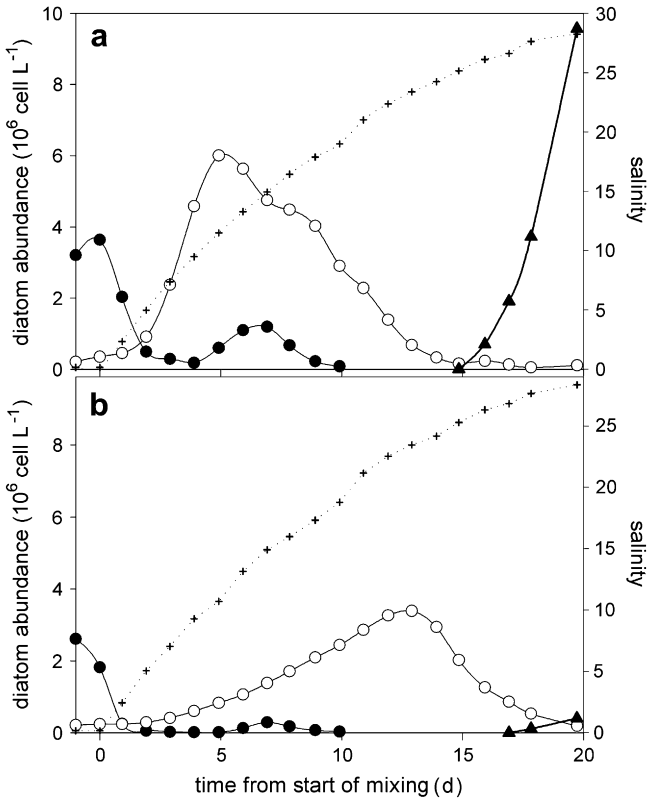

Fig. 3. Cell abundance evolution of the diatoms *A. formosa* (●), *C. meneghiniana* (○) and *S. costatum* (▲) from the beginning of freshwater and seawater mixing in the cultures at high light (a) and low light (b). The dotted line shows the evolution of salinity in each culture.

dominance of *Skeletonema costatum*. The initial drop of *Asterionella formosa* abundance was faster at low light and the mid-salinity peak of the diatom occurred at the same time as at high light but was much lower. *Cyclotella meneghiniana* reached its maximal abundance on day 13 when salinity was 23 i.e. much higher than under high light but in agreement with the large salinity tolerance of the species (Fig. 2).

DSi exhaustion was observed for the two light conditions (Fig. 4) but this occurred much earlier at high light (around

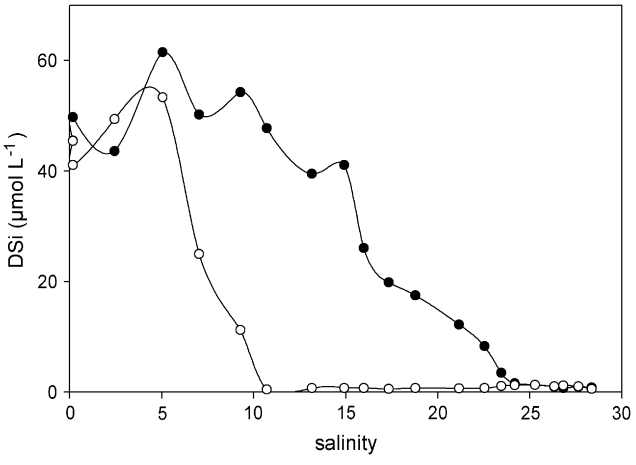

Fig. 4. DSi concentration versus salinity in the high light (○) and low light (●) cultures during the mixing of freshwater and seawater.

day 12) than at low light (day 24). DSi depletion coincided with the maximum abundance of *Cyclotella meneghiniana* (Figs. 3 and 4) and to a less extent with the second peak of *Asterionella formosa* under high light. The shape of the DSi curves (Fig. 4) also suggests some $bSiO_2$ dissolution from dead diatom frustules at the beginning of the experiment.

The net sedimentation of frustules per liter of freshwater (Sed_F) along the mixing was calculated as an indicator of Si removal from the water column (Fig. 5). For each species, it corresponds to the negative values of the variations in frustule concentration (F_t), corrected by freshwater dilution and by input from seawater:

$$\underset{t-1\to t}{\mathrm{Sed}_F} = \left(F_t - F_{t-1}\frac{S_{\mathrm{mar}} - S_t}{S_{\mathrm{mar}} - S_{t-1}} - \underset{t-1\to t}{F_{\mathrm{in}}}\right)\cdot\frac{S_{\mathrm{mar}}}{S_{\mathrm{mar}} - (S_{t-1} + S_t)/2}$$

Where S_t and S_{mar} are the salinity in the water column at time t and seawater salinity respectively and F_{in} is the input of frustules from the seawater culture (c) (only for *Skeletonema costatum*). Because of the very low value of F_{in} and the continuous increase in frustule concentration of *S. costatum* at the end of the experiment, no net frustule sedimentation could be measured for this species.

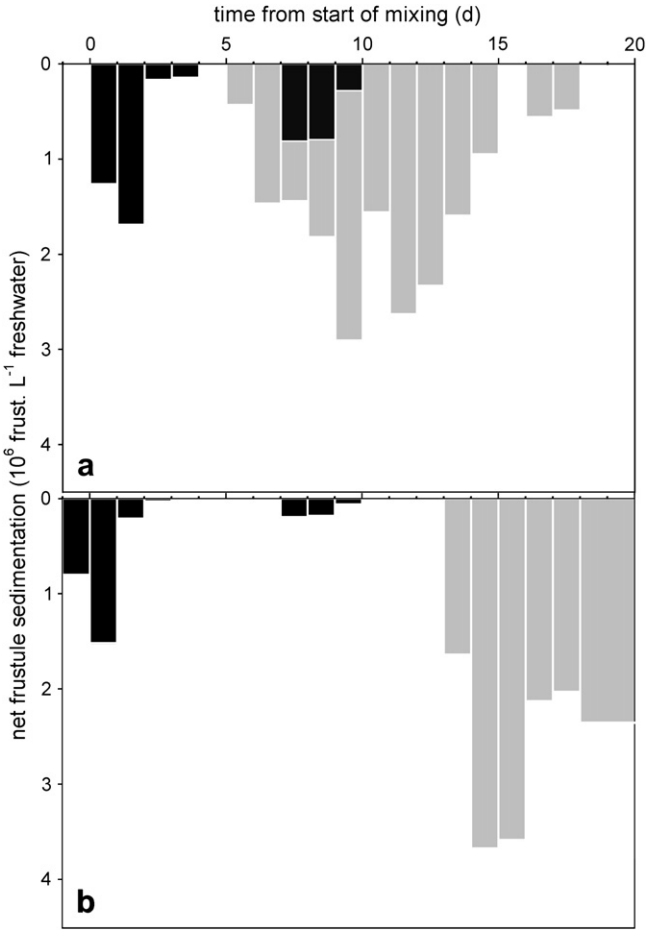

Fig. 5. Diatom frustule net sedimentation at high light (a) and low light (b) estimated from time variations in frustule concentration of *A. formosa* (black bars) and *C. meneghiniana* (grey bars).

The net sedimentation of *Asterionella formosa*'s frustules was distributed at the beginning and in the middle of the salinity gradient in relation with the observed two maxima of abundance (Figs. 3 and 5). The first net frustule sedimentation event associated to *A. formosa*'s decline was quite similar for the two light conditions whereas the second one was much reduced at low light (Fig. 5). At high light, the net sedimentation of *Cyclotella meneghiniana*'s frustules lasted from day 5 to 18 with a maximum between days 9 and 13. On the contrary, net sedimentation at low light was concentrated in the last days of the experiment. The comparison of the distribution of frustule net sedimentation between the two light levels suggests a faster removal of Si from freshwater along the mixing where the irradiance was higher.

3.2. Modelling Si transformations in an estuarine mixing zone

Si transformations in estuarine mixing zones were further investigated by the construction and use of a conceptual model derived from the previous experiment and applied to the particular case of the surface layer in a highly stratified estuary. Si transformations and Si removal from freshwater via $bSiO_2$ sinking into the bottom marine layer were studied in relation to variations in some model parameters (dissolution, sedimentation and water mixing rates) and constraints (turbidity, $bSiO_2$ river load and marine $bSiO_2$ concentration).

3.2.1. Model construction

The model describes Si fluxes in the surface layer of an idealized, highly stratified estuary at steady flow (Fig. 6). The river water discharging at the head of this estuary (flux R) is progressively diluted by entrainment of underlying seawater along its transport toward the mouth of the estuary and finally discharges into the sea (Q_{out}) as brackish water after a transit time T_{trs}. The marine layer receives a residual input Q_{sea} from the adjacent sea and the entrainment of seawater through the marine-brackish water interface (q_{sea}) is assumed to be constant. The surface layer is assumed to be vertically and laterally well-mixed and has a constant depth (Z_{mix}) from the head to the mouth of the estuary. The model calculates Si transformations and removal in an elementary volume contained in a cross section of the surface layer flowing down to the sea (Fig. 6).

The state variables and the Si fluxes are shown on the model diagram of Fig. 7. The variable $bSiO_2$ stands for the biomass (in µmol Si L^{-1}) of three key diatom groups pointed by the previous experiments: the stenohaline (SRD) and euryhaline (ERD) river diatoms and the euryhaline coastal diatoms (ECD). Detrital $bSiO_2$ (det $bSiO_2$) represents $bSiO_2$ remains from dead diatoms. SPM corresponds to all suspended particulate matter in the water column except diatom biomass. The DSi, $bSiO_2$ and det $bSiO_2$ variables are each subdivided into a marine and riverine one in order to trace the fate of river Si and disentangle its removal from that of marine Si. The following processes are considered (Fig. 7): diatom growth and mortality, sedimentation, dilution, $bSiO_2$ dissolution and

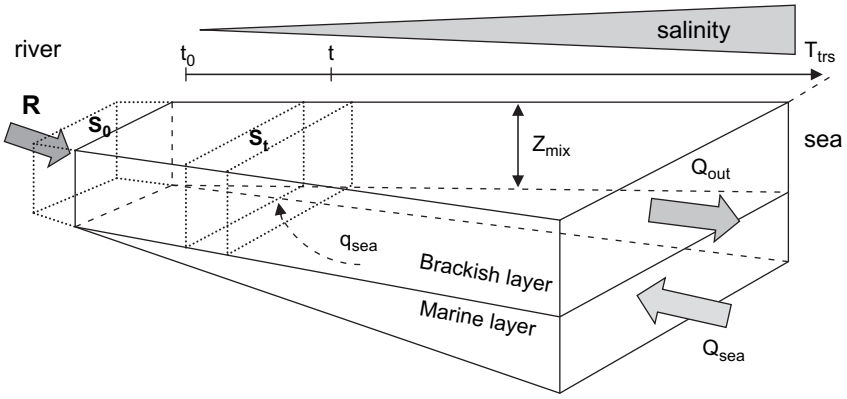

Fig. 6. Schematic representation of an idealized estuary of the highly stratified type corresponding to the developed Si model. The steady residual flows at the boundaries are the river discharge R, the tidal marine input Q_{sea} and the estuarine output to the sea Q_{out}. The model represents Si transformations in a water mass of salinity S flowing from the river mouth to the sea and receiving by entrainment a flux of seawater q_{sea} at the marine-brackish layer interface. This water mass reaches the sea after a transit time T_{trs}.

Si inputs from the marine layer, the latter being only composed of marine DSi (DSi_{mar}) and euryhaline coastal diatoms ($bSiO_{2\ mar}$).

Each state variable is diluted at a constant rate D by the input of water from the marine layer. The initial values of the state variables i.e. upstream the estuarine mixing zone, are listed in Table 1. They correspond to a little turbid river with DSi and $bSiO_2$ concentrations close to the global means (Conley, 1997) and which contains 5-fold less euryhaline than stenohaline diatoms. Processes taking place in the marine layer are not represented in the model. Thus, DSi_{mar}, $bSiO_{2\ mar}$, salinity and SPM_{mar} are kept constant in the marine layer (Table 1) which assumes that the marine layer is initially homogeneous when the mixing starts and that settled matter from the surface layer to the marine layer can not return to the same water mass where it comes from. Model parameters are reported in Table 2.

The boundary input fluxes are constant and the other Si fluxes are mostly described by a first order equation whose rate constant is indicated in Table 2. Only diatom growth and mortality have more complex expressions. Physiological parameters are identical for each diatom group except the Si half-saturation constant for growth (K_{Si}) which is lower for coastal diatoms (Paasche, 1980b) and the parameters of the salinity-dependant mortality function (S_{opt} and K_{sal}) which are adapted to the salinity tolerance of each group.

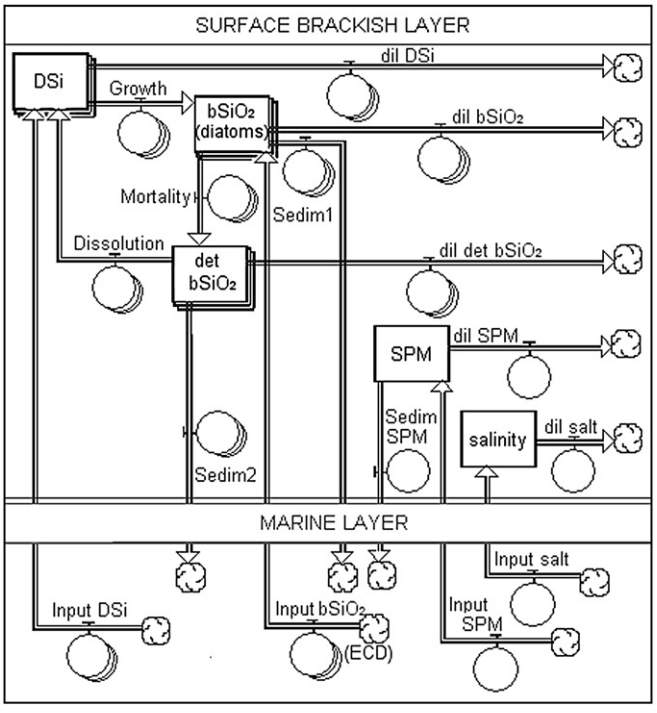

Fig. 7. Diagram of the estuarine Si model simulating the variations in concentration of three forms of Si (DSi, diatom $bSiO_2$ and detrital $bSiO_2$) and of the suspended particulate matter (SPM) and the evolution of salinity in the surface brackish layer of a highly stratified estuary during mixing with seawater. The rectangles correspond to the state variables and the arrows are the Si fluxes between them. The ''dil'' fluxes express the dilution of each state variable by the input of seawater; ''Sedim'' means sedimentation.

Table 1
Initial values of the model state variables and boundary conditions

State variables	Acronym	Unit	Initial value
Dissolved silica concentration	DSi	µmol Si L^{-1}	100
Biogenic silica concentration of stenohaline river diatoms (SRD)	$bSiO_{2\ SRD}$	µmol Si L^{-1}	10
Biogenic silica concentration of euryhaline river diatoms (ERD)	$bSiO_{2\ ERD}$	µmol Si L^{-1}	2
Biogenic silica concentration of euryhaline coastal diatoms (ECD)	$bSiO_{2\ ECD}$	µmol Si L^{-1}	0
Detrital biogenic silica concentration	det $bSiO_2$	µmol Si L^{-1}	0
Suspended particulate matter concentration	SPM	mg L^{-1}	20
Salinity	S		0
Boundary conditions	**Acronym**	**Unit**	**Value**
Marine layer salinity	S_{mar}		33
Marine layer DSi concentration	DSi_{mar}	µmol L^{-1}	10
Marine layer $bSiO_2$ concentration (ECD)	$bSiO_{2\ mar}$	µmol L^{-1}	2
Marine layer SPM concentration	SPM_{mar}	mg L^{-1}	5

Table 2
Si model biogeochemical (a) and physical (b) parameters. Sources: (a) Roubeix (2007); (b) Tilman and Kilham (1976); (c) Patel et al. (2004); (d) Shafik et al. (1997); (e) Van Cappellen et al. (2002); (f) Sarthou et al. (2005); (g) Soetaert et al. (1994); (h) Cloern (1987)

	Parameters	Acronym	Unit	Model values	Literature range
a	Maximal growth rate μ_{max}	μ_{max}	d^{-1}	1	0.7–0.9[a]; 0.8–1.5[b,c,d]
	Si half saturation constant for growth	K_{si}	µmol L^{-1}	2 (SRD,ERD); 0.5 (ECD)	1–4[b]; 3.9 ± 5[e]
	Light adaptation parameter	I_k	µmol quanta m^{-2} s^{-1}	100	70–150[a]; 95 ± 40[e]
	Mortality rate at optimal salinity	M	d^{-1}	0.1	0.005–0.24[e]
	Optimal salinity	S_{opt}		0 (SRD); 17(ERD); 37(ECD)	
	Salinity sensitivity parameter	K_{sal}		1.6(SRD); 0.026(ERD); 0.017(ECD)	
	$bSiO_2$ dissolution rate	R_{diss}	d^{-1}	0.04	0.00–0.08[a]; 0.04[e]
	Sinking velocity of $bSiO_2$	V_{sed}	m d^{-1}	0.15 (diatoms), 0.6 (det $bSiO_2$)	0.1–0.6[a]; 0.2–0.6[c]; 0.1–1.5[f]
b	Brackish layer depth	Z_{mix}	m	3	
	Surface irradiance	I_0	µmol quanta m^{-2} s^{-1}	500	
	Brackish layer dilution rate	D	d^{-1}	0.13	
	SPM sinking velocity	V_{SPM}	m d^{-1}	0.1	
	Light extinction coefficient	K_{ext}	m^{-1}	$K_0 + K_{SPM}$ SPM + K_{cel} c $bSiO_2$	
		K_0	m^{-1}	0.59[g]	
		K_{SPM}	m^{-1} (mg L^{-1})$^{-1}$	0.06[h]	
		K_{cel}	m^{-1} (µg Chl *a* L^{-1})$^{-1}$	0.012[c]	
		c	µg Chl *a* µmol $bSiO_2^{-1}$	2.3[a]	

Diatom growth is controlled by light and DSi availability as follows:

$$\text{Growth}_{d,s} = \mu_{\max_d} \frac{\text{DSi}}{K_{\text{Si}_d} + \text{DSi}} \left(1 - e^{-I/I_k}\right) \text{bSiO}_{2_d} \frac{\text{DSi}_s}{\text{DSi}}$$

where d refers to either SRD, ERD or ECD and s to the riverine or marine origin of Si, μ_{max} is the maximal growth rate and K_{Si} the half saturation constant for growth.

I is the average irradiance in the brackish layer defined by:

$$I = \frac{I_0}{K_{\text{ext}} Z_{\text{mix}}} \left(1 - e^{-K_{\text{ext}} \cdot Z_{\text{mix}}}\right)$$

Where I_0 is the surface irradiance and K_{ext} the light extinction coefficient depending on SPM and $bSiO_2$ concentrations in the surface brackish layer (Table 2).

Diatom mortality depends on salinity assuming that mortality is as high as the diatom group d is far from its growth salinity optimum S_{opt_d}:

$$\text{Mortality}_{d,s} = M_d f_d(S) \text{bSiO}_{2_{d,s}}$$

Where M_d is the mortality rate at optimal salinity and f_d is a parabolic function with a minimum of 1 at S_{opt_d}:

$$f_d(S) = 0.5 K_{\text{sal}_d} \left(S - S_{\text{opt}_d}\right)^2 + 1$$

K_{sal_d} is a parameter which expresses the sensitivity of the diatom group d to salinity. The parameters S_{opt_d} and K_{sal_d} were estimated for each diatom group (Table 2) by fitting the computed relative change in net growth (growth minus mortality) of each diatom group to the growth rate versus salinity data of *Asterionella formosa*, *Cyclotella meneghiniana* and *Skeltonema costatum* (Fig. 2), used here as model for SRD, ERD and ECD respectively.

Finally, the cumulated removal of Si from freshwater (R_{riv} in %) at time t from the beginning of the mixing (t_0) was calculated from the comparison between the value of the total initial riverine Si (Si_{tot_r}) and the value expected retrospectively at t_0 assuming a conservative mixing of the total riverine Si present at time t and salinity S_t:

$$R_{\text{riv}}(t) = 1 - \left[\left(\text{DSi}_r + \sum_d \text{bSiO}_{2_{d,r}} + \text{det bSiO}_{2_r} \right) \times \frac{S_{\text{mar}}}{(S_{\text{mar}} - S_t)} \right] \Big/ \text{Si}_{\text{tot}_r}$$

The removal rate of Si from freshwater (R'_{riv} in % d^{-1}) can then be derived from R_{riv}:

$$R'_{\text{riv}}(t) = \frac{\mathrm{d}R_{\text{riv}}(t)}{\mathrm{d}t}$$

3.2.2. Model results

Model simulations of Si transformations during the mixing of freshwater and seawater were performed using STELLA software (HPS). The state equations were solved using the Euler's method with a time step of 0.01 day. The simulation time was 20 days. The model results are shown on Fig. 8 and Table 3 and compare simulations obtained with the reference conditions and those obtained by changing parameters and initial conditions reported in Tables 1 and 2. As a general trend, the simulated evolution of the biomass of each diatom group along the salinity gradient (Fig. 8a) is similar to that observed for each diatom species in the mixing experiment (Fig. 3). The main differences are the absence in the model of a second peak of SRD in the middle of the salinity gradient and an earlier increase of the biomass of ECD (Figs. 3 and 8). The removal rate of Si from freshwater during mixing (Fig. 8a) shows a bimodal curve with a first moderate peak at 3% d^{-1} on day 2 associated to the decline of SRD and

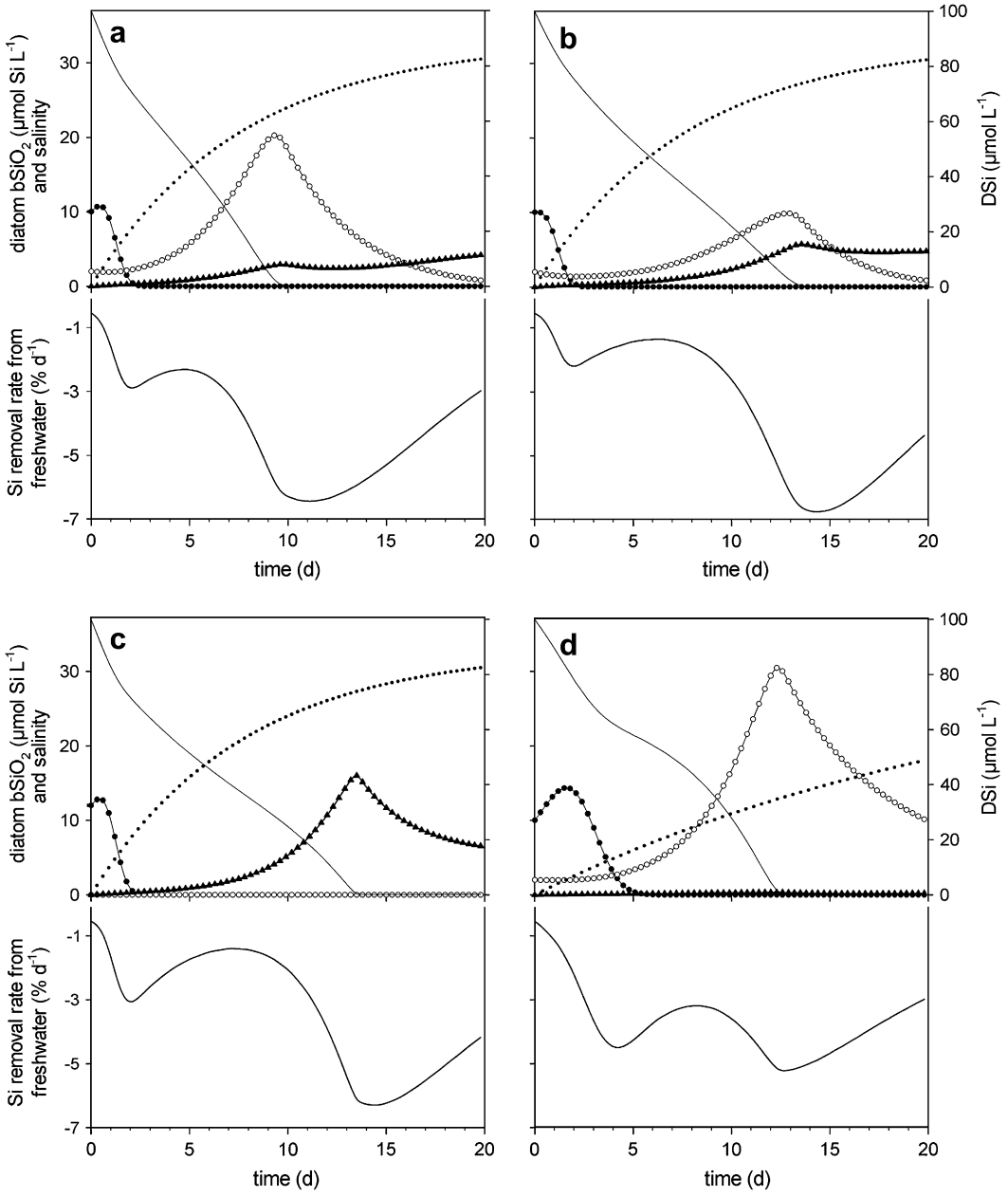

Fig. 8. Model simulations showing the evolution of the $bSiO_2$ concentration of SRD (●), ERD (○) and ECD (▲) (upper panel) and the Si removal rate from freshwater (R'_{riv}) (lower panel) during the mixing of freshwater and seawater in the reference conditions (a), when the turbidity of the river water is increased to an SPM concentration of 60 mg L^{-1} (b), in the case where all river diatoms are SRD (c) and when the dilution rate of the brackish layer is decreased to 0.4 d^{-1} (d). In the graphs of the model variables (upper panel), the dotted line shows the evolution of salinity and the solid line the evolution of DSi concentration.

a second larger peak at 6% d^{-1} on day 11 following the prominent development of ERD.

3.2.2.1. Sensitivity analysis on initial and boundary conditions. The effect of light availability for diatom growth and Si removal in the brackish layer was investigated by running the model with different initial concentrations in SPM corresponding to more or less turbid river waters. Light availability in the water column indeed increases as the SPM discharged by the river settles down and is diluted by less turbid marine waters. As an example, Fig. 8b shows a simulation obtained when the initial SPM is increased from 20 to 60 mg L^{-1} which corresponds to a mean light irradiance decrease from 80 to 35 µmol quanta m^{-2} s^{-1} in the water column at the beginning of the mixing. As observed in the mixing experiment with *Cyclotella meneghiniana* (Fig. 3), the decreased light availability delays and decreases the maximal biomass reached by ERD (Figs. 8a,b). ECD reach their highest biomass at the end of the mixing (Fig. 8) but unlike *Skeletonema costatum* in the mixing experiment (Fig. 3), the increase in biomass is larger when the average light level during mixing is lower (Figs. 8a,b). Higher initial SPM concentration also postpones DSi depletion for 4 days compared to the reference simulation. The increased turbidity has no effect on the simulated SRD

Table 3
Sensitivity analysis showing the effect of ±50% variations of model parameters and initial and boundary conditions on the cumulated removal of Si (R_{riv}) from freshwater after 5 and 15 days

Parameters/initial conditions	Reference value		% change of R_{riv}	
			After 5 days	After 15 days
SPM	20	−50%	+15.5	+7.1
		+50%	−17.3	−15.1
% ERD[a]	17	−50%	−1.5	−6.6
		+50%	+2.4	+5.7
% $bSiO_2$ in river[b]	11	−50%	−44.0	−12.4
		+50%	+68.4	+13.0
D	0.13	−50%	+15.5	−11.3
		+50%	−6.6	+9.9
R_{diss}	0.04	−50%	+2.7	+1.9
		+50%	−2.5	−1.8
V_{sed}	0.15 and 0.6	−50%	−40.9	−32.3
		+50%	+28.5	+17.5
Z_{mix}	3	−50%	+103.7	+42.3
		+50%	−37.6	−36.4
$bSiO_{2\ mar}$	2	−50%	−1.0	−1.4
		+50%	+1.0	+1.3
$bSiO_{2\ mar}$ (no ERD)[c]	2	−50%	−1.1	−21.5
		+50%	+1.1	+13.0

[a] Variations of the proportion of ERD in the river without modification of the total $bSiO_2$ load.
[b] Variations of the proportion of $bSiO_2$ in the total Si river load.
[c] In this case, the simulation where there are no ERD in the river was taken as reference (Fig. 8c).

which die soon after the beginning of the mixing so that the time interval between the peaks of Si removal rate from freshwater is increased, the second maximum occurring only on day 14 (Fig. 8b). The effect of river turbidity on the dynamics of Si removal can also be seen in Table 3 where a doubling or a reduction by half of SPM leads respectively to a decrease or an increase of the total Si removal from freshwater on days 5 and 15 (Table 3).

The consequences of changes in the total biomass and composition of the river diatom community were analyzed by modifying the initial value of the $bSiO_2$ in the model (Fig. 8c, Table 3). Fig. 8c presents a simulation obtained when river diatoms are composed of SRD only. Results show that when ERD are absent, the depletion of DSi is due to ECD which reach a maximal biomass on day 13, i.e. 4 days later than ERD in the reference run (Fig. 8a). ECD are responsible of the second larger peak of Si removal which is delayed until day 14 as in Fig. 8b. Further sensitivity analysis on the proportion of ERD in the river diatom community suggests that Si removal from freshwater is as fast as ERD biomass is high (Table 3). Also, a high sensitivity of the removal of Si from freshwater to the proportion of living diatom $bSiO_2$ in the river Si load was demonstrated by model simulations, a higher $bSiO_2$ load from the river leading to faster riverine Si removal in the estuary (Table 3). Finally, the $bSiO_2$ concentration of the marine end-member ($bSiO_{2\ mar}$) determining marine diatom (ECD) input to the estuarine surface layer was tested (Table 3). The riverine Si removal from the surface layer is not sensitive to the variations of $bSiO_{2\ mar}$. However, if the situation where there is no ERD (Fig. 8c) is taken as the reference, variations of this parameter show considerable influence on Si removal on day 15. A higher concentration of coastal diatoms in the marine layer results in a faster removal of Si from freshwater especially at the end of mixing.

3.2.2.2. Sensitivity analysis on parameters. Fig. 8d shows the effect of a three-fold lower dilution rate D on the simulated diatom succession and on Si removal along the mixing. The lower rate of salinity increase allows a larger development of SRD and subsequent DSi uptake (Fig. 8d). The peak of ERD occurs a bit later compared to the reference run (Fig. 8a) and depletes DSi. ECD do not appear in the water column during the 20 first days of mixing. In this model scenario, the two peaks of Si removal on days 4 and 12 have the same importance reflecting the larger contribution of SRD (Fig. 8d). Further model simulations show that the variations of the parameter D which can be the consequence of variations in the tidal volume (Q_{sea}) entering the estuary have opposite effects on the cumulated Si removal on days 5 and 15 (Table 3). The sinking velocity of either living or lysed diatoms (V_{sed}) and the depth of the surface brackish layer (Z_{mix}) have the strongest influence on Si removal from freshwater (Table 3) and are respectively positively and negatively correlated to Si removal. Interestingly, the variations of the dissolution rate of diatom $bSiO_2$ have very little consequence on Si removal in the reference conditions.

4. Discussion

4.1. Si biogeochemical processes in an estuarine salinity gradient

4.1.1. Experimental approach

The construction of a continuous salinity gradient provides the most realistic conditions to study the behavior of diatoms in an estuarine mixing zone. It is preferred to the instantaneous mixing of freshwater with saline water which exposes algae to sudden salinity changes (Doering et al., 1995; Yin et al., 2000; Ragueneau et al., 2002; Lionard et al., 2005). Indeed, not only the absolute value but also the rate of salinity change might affect phytoplankton physiology (Flameling and Kromkamp, 1994). In our mixing experiment, the two freshwater diatoms *Asterionella formosa* and *Cyclotella meneghiniana* experienced a gradual salinity increase while the coastal species *Skeletonema costatum* was directly injected in lower salinity water. This type of mixing is realistic for stratified estuaries in which entrainment of saline water brings marine phytoplankton upwards into the brackish surface layer (Yin et al., 2000). In mixed estuaries, the diffusion of seawater into the estuary might expose marine species to a gradual salinity decrease. Thus, our experimental design rather represents the mixing of river water and seawater in a highly stratified estuary. Nonetheless, the way seawater is mixed with river water should not have important consequences for *S. costatum* since this species was shown to adapt well to high salinity fluctuations (Rijstenbil, 1988). Similarly, *C. meneghiniana* exhibited a good tolerance to salinity rise and its growth rate seemed

only determined by the instantaneous salinity level (Fig. 2) and DSi availability, suggesting a fast osmoregulatory mechanism. On the contrary, *A. formosa* was sensitive to salinity change as shown by the very different growth pattern of the diatom in a salinity gradient (Fig. 3) and after inoculation at constant salinities (Fig. 2). The difference suggests that a gradual salinity increase does not trigger cell plasmolysis but blocks growth during an adaptation phase after which diatoms can develop at higher salinities. The gradual salinity increase could be a signal for the cell leading to the activation of osmoregulation processes like the production of organic osmotica (Erdmann and Hagemann, 2001). This would explain why *A. formosa* was still able to grow at salinity >10 in the experimental salinity gradient (Fig. 3) whereas it could not grow when directly inoculated from salinity 0 to salinity 5 or 10 (Fig. 2). In the mixing experiment, *A. formosa* could adapt to salinity increase only up to salinity 15 beyond which the diatom did not grow whatever the light conditions were even when DSi was still available (Fig. 3b).

The mixing of freshwater and seawater during 20 days led to the accumulation of detrital $bSiO_2$ at the bottom of the flasks. The settled $bSiO_2$ in turn dissolved along the mixing and Si was then re-injected into the same water mass where it came from. This is in contradiction with the idea that the studied water mass is flowing from river to sea as it is diluted with seawater in a stratified estuary. This experimental artifact precluded the estimation of Si uptake by diatoms from the variations in DSi concentration and therefore that of Si removal by sedimentation from the variations in $bSiO_2$ concentrations. The net frustule sedimentation can be an indicator of Si removal from freshwater, keeping however in mind that the Si content of the frustules can be different between the two freshwater species (*Cyclotella meneghiniana* being usually more silicified than *Asterionella formosa*), that it might change due to physiological stress of the cells (Martin-Jézéquel et al., 2000) and that some Si could be of marine origin or recycled from the bottom of the flasks. However, the net sedimentation of diatom frustules allows a comparison of the dynamics of Si removal from freshwater in the two light conditions.

4.1.2. Modelling approach

The construction of a Si model based on the mixing experiment allowed calculation of the riverine Si removal from the surface layer of an idealized stratified estuary. The model uses usual mathematical expressions for the main Si processes and the biological parameters were estimated from existing literature or based on our own laboratory measurements. The description of the salinity effect on diatom growth was the most difficult. Salinity change causes osmotic stress to algal cells which results in higher mortality. Thus the salinity effect on phytoplankton growth is generally expressed as a salinity-dependant function in the mortality rate expression (Soetaert et al., 1994; Romero et al., 2003). In this study, the parabolic mortality function was derived from measured growth rates of acclimated diatoms at constant salinity. Thus, such a mortality description ignores any adaptation process. The case of *Asterionella formosa* shows that more knowledge is needed about the adaptation mechanisms of diatoms to specify the salinity effect in a model. By now the Si model relies on the existence of an average absolute salinity limit for the different diatom groups and particularly stenohaline river diatoms (SRD) do not grow over salinity 4 (Fig. 2). The simulation of ERD evolution in the salinity gradient is satisfying considering the similar responses to salinity change and decrease in light availability of *Cyclotella meneghiniana* in the mixing experiment and ERD in the model (Figs. 3 and 8). Concerning ECD, the main difference with the experiment consists of the faster increase in biomass when the average light level during mixing is lower. This can be explained by the combined effect of the surplus of available DSi due to the lower development of the ERD and the light increase toward higher salinities which is considered in the model only.

The catalyzing effect of salinity on $bSiO_2$ dissolution (Yamada and D'Elia, 1984; Roubeix, 2007) was not implemented in the model because this effect is not well known yet and because the model was not sensitive to variations in the dissolution rate parameter (R_{diss}, Table 3) in the given estuarine conditions.

4.2. Main factors controlling Si removal from freshwater

4.2.1. Freshwater transit time

The transit time T_{trs} of freshwater in the estuarine mixing zone corresponds to its flushing time T_f (Sheldon and Alber, 2002; Humborg et al., 2003):

$$T_{trs} = T_f = \frac{V_f}{R}$$

Where V_f is the volume of freshwater in the mixing zone and R the river discharge. Time in the experimental and model results can be interpreted either as the age of freshwater (Monsen et al., 2002) at a given transit time or as the transit time from the beginning of mixing to the mouth of the estuary for different river discharges (R). Clearly our simulations show that the shorter the transit time is the lower is Si removal in the estuarine mixing zone (Fig. 8). This is because DSi uptake and $bSiO_2$ sinking are essentially time dependant. Similarly the water residence time in estuaries was shown to be the main factor controlling nitrogen retention on an annual basis (Dettmann, 2001). However, the magnitude of the transit time effect on riverine Si removal depends on other factors affecting diatom DSi uptake and sedimentation. For instance, the extent to which Si removal increases with transit time is lower when light availability is decreased because of high turbidity (Fig. 8b).

4.2.2. Turbidity and light availability

High turbidity in estuaries reduces primary production because of photosynthesis limitation by low light penetration into the water column (Cloern, 1987). Thus in estuaries, the part of Si removal resulting from the development and settling of diatom biomass should be lower in turbid waters. This is confirmed by the experimental and model results obtained

for different irradiances or turbidities (Figs. 5 and 8a,b, Table 3). The first removal phase until day 4 is not much affected by light availability as it corresponds to sedimentation of stenohaline diatoms which have a very limited development in the salinity gradient. Then, the second phase of Si removal clearly occurs earlier when available light is higher in both the mixing experiments (Fig. 5) and the model simulations (Figs. 8a,b). A long transit time in the estuary can therefore compensate the effect of high turbidity on riverine Si removal. Thus, transit time and turbidity are interacting factors and can probably explain a large part of variations in silica removal from freshwater in estuaries.

4.2.3. Mixed layer depth and halocline

A deeper mixed layer reduces riverine Si removal because of the lower mean light available for diatoms in the layer and a longer sedimentation time to reach the underlying marine layer. The higher impact on Si removal of Z_{mix} compared to V_{sed} reflects this double effect (Table 3). $bSiO_2$ sedimentation into the marine layer can be reduced in highly stratified estuaries because of the trapping of sediments in an interface layer between the surface and the marine layer (e.g. Ebre estuary, Ibanez et al., 1999). In the highly stratified Krka estuary, Legovic et al. (1996) estimated that only one third of $bSiO_2$ in the surface brackish layer could sink through the sharp halocline. The sensitivity analysis on the sinking velocity parameter of $bSiO_2$ (V_{sed}) points the important consequence that can have this physical barrier on Si fluxes to the sea (Table 3).

4.2.4. Tides and mixing

The mixing of freshwater and seawater in an estuary is mainly regulated by the river water flow and the magnitude of the tidal currents (Hansen and Rattray, 1966). In a stratified estuary, at a given river discharge R, an increased tidal volume Q_{sea} may increase current shear at the interface between the two layers and enhance saline water injection into the surface brackish layer (Kay and Jay, 2003). This results in a higher dilution rate D of freshwater and a higher salinity S_{out} at the mouth of the estuary in agreement with the Knudsen formula: $S_{out} = S_{sea}Q_{sea}/(R + Q_{sea})$ (Fig. 6). A lower tidal regime would result in exactly the opposite. The effect of the dilution rate of freshwater on riverine Si removal is complex (Table 3, Fig. 8d). The dilution rate determines the steepness of the salinity gradient and consequently the time available for SRD to develop in a restricted salinity range. However, it also controls the dilution rate of riverine SPM and the average turbidity in the surface brackish layer which mostly affects the Si uptake by euryhaline diatoms. This explains the opposite effect of D on Si removal from freshwater at the beginning and at the end of mixing (Table 3).

4.3. Importance of estuarine boundary conditions

The removal of Si from freshwater in an estuary depends also on the $bSiO_2$ present in the two adjacent systems preceding and following estuaries in the land-ocean continuum: river and sea.

The percentage of $bSiO_2$ in the total Si discharged by the river influences Si removal in the estuary (Table 3). This means that higher Si removal should be expected when high diatom biomass is already present in the river. Particularly, higher Si removal might take place in an estuary during the period of diatom blooms in a river characterized by a marked seasonality (e.g. in Sullivan et al., 2001; Cugier et al., 2005). Moreover, the composition of the diatom community entering the estuarine mixing zone has also consequences on estuarine Si removal. Indeed, an increased proportion of ERD in the river diatom community can result in a higher estuarine Si removal (Table 3). Euryhaline diatoms are not only found in systems with fluctuating salinity like estuaries but they are also present in the plankton of rivers and lakes among stenohaline diatoms. For example, the euryhaline diatom *Cyclotella meneghiniana* is reported in many rivers all over the world (Shafik et al., 1997; Finlay et al., 2002). Consequently it also appears downstream in estuaries among SRD like *Asterionella formosa* (Muylaert and Sabbe, 1999). The proportion of ERD at the river mouths could potentially be high but its overall contribution remains today difficult to assess.

In some cases, the abundance of diatoms in the marine layer can positively affect riverine Si removal. Particularly when no ERD is loaded by the river into the mixing zone, the input of a higher amount of ECD into the brackish layer allows a faster consumption of DSi and a higher removal of riverine Si (Table 3). This effect is however decreased when ERD can develop in the salinity gradient. This shows that riverine Si removal in an estuary can be facilitated when the diatom biomass in the adjacent sea is higher.

4.4. The estuarine filter

The removal of Si from freshwater in estuarine mixing zones estimates the filtering capacity of estuaries for the continental reactive Si fluxes (DSi and $bSiO_2$). The magnitude of the filter determines the immediate contribution of continental Si to the coastal ecosystem. However, the estimation of the net Si enrichment of the coastal sea has to account for the part of marine silica trapped in the estuary which has to be subtracted from the continental Si flux. For example, in the reference simulation (Tables 1 and 2), one third of the total settled $bSiO_2$ after 20 days did not come directly from the river system but from estuarine recycling and marine input.

Among the successive filter systems along the land-ocean continuum, estuaries are intermediate between rivers and lakes as regard to the residence time and the geomorphology (Billen et al., 1991). But the gradual change in salinity leading to the death and sedimentation of the stenohaline planktonic species is a unique property of the estuarine filter. There might be two components in the silica filter effect of estuaries: the first one is linked to the mortality and sedimentation of river diatoms experiencing osmotic stress at the beginning of the salinity gradient and the second one is related to the uptake of river DSi by euryhaline diatoms during the transit time of freshwater in the estuary. In the model simulations, these two components can be identified by two distinct peaks of the Si removal

rate along the time of mixing (Fig. 8). The prevailing factors controlling the extent of the first component of the estuarine filter might be the total $bSiO_2$ discharged by the river and the proportion of euryhaline species in the river diatom community. Since the second component of the estuarine filter is linked to the growth of diatoms resistant to salinity change, the main factors controlling it might be the same as those controlling Si retention in lakes: thus residence time, turbidity or photic depth and nutrient availability should be the most determining factors.

Acknowledgments

The present work has been performed in the scope of the EU Research Training Network Si-WEBS and of the AMORE-III and TIMOTHY projects funded respectively by the Science for Sustainable Development and by the Interuniversity Attraction Poles Programme-Belgian State-Belgian Science Policy. Vincent Roubeix had a doctoral fellowship funded by EU in the scope of Si-WEBS. Jean-Yves Parent and Koenraad Muylaert are thanked for their help with diatom cultures.

References

Ahel, M., Barlow, R.G., Mantoura, R.F.C., 1996. Effect of salinity gradients on the distribution of phytoplankton pigments in a stratified estuary. Marine Ecology Progress Series 143, 289–295.

Bien, G.S., De Contois, D.E., Thomas, W.H., 1958. The removal of soluble silica from fresh water entering the sea. Geochimica et Cosmochimica Acta 14, 35–54.

Billen, G., Lancelot, C., Meybeck, M., 1991. N, P and Si Retention along the aquatic continuum from land to ocean. In: Mantoura, R.F.C., Martin, J.-M., Wollast, R. (Eds.), Ocean Margin Processes in Global Change. John Wiley & Sons Ltd, Chichester, pp. 19–44.

Chou, L., Wollast, R., 2006. Estuarine silicon dynamics. In: Ittekot, V., Unger, D., Humborg, C., Tac An, N. (Eds.), The Silicon Cycle- Human Perturbations and Impacts on Aquatic Systems. Island Press, Washington, pp. 93–120.

Cloern, J.E., 1987. Turbidity as a control on phytoplankton biomass and productivity in estuaries. Continental Shelf Research 7, 1367–1381.

Conley, D.J., 1997. Riverine contribution of biogenic silica to the oceanic silica budget. Limnology and Oceanography 42, 774–777.

Cugier, P., Billen, G., Guillaud, J.F., Garnier, J., Ménesguen, A., 2005. Modelling the eutrophication of the Seine Bight (France) under historical, present and future riverine nutrient loading. Journal of Hydrology 304, 381–396.

DeMaster, D.J., Smith Jr., W.O., Nelson, D.M., Aller, J.Y., 1996. Biogeochemical processes in Amazon shelf waters: chemical distributions and uptake rates of silicon, carbon and nitrogen. Continental Shelf Research 16, 617–643.

Dettmann, E.H., 2001. Effect of water residence time on annual export and denitrification of nitrogen in estuaries: a model analysis. Estuaries 24, 481–490.

Doering, P.H., Oviatt, C.A., Nowicki, B.L., Klos, E.G., Reed, L.W., 1995. Phosphorus and nitrogen limitation of primary production in a simulated estuarine gradient. Marine Ecology Progress Series 124, 271–287.

Egge, J.K., Aksnes, D.L., 1992. Silicate as regulating nutrient in phytoplankton competition. Marine Ecology Progress Series 83, 281–289.

Erdmann, N., Hagemann, M., 2001. Salt acclimation of algae and cyanobacteria: a comparison. In: Rai, L.C., Gaur, J.P. (Eds.), Algal Adaptation to Environmental Stresses. Springer, Berlin, pp. 323–361.

Finlay, B.J., Monaghan, E.B., Maberly, S.C., 2002. Hypothesis: the rate and scale of dispersal of freshwater diatom species is a function of their global abundance. Protist 153, 261–273.

Flameling, I.A., Kromkamp, J., 1994. Responses of respiration and photosynthesis of *Scenedesmus protuberans* Fritsch to gradual and steep salinity increases. Journal of Plankton Research 16, 1781–1791.

Grasshoff, K., Erhardt, M., Kremling, K., 1983. Methods of Seawater Analysis. Verlag Chemie, Weinheim, 419 pp.

Guillard, R.R.L., Lorenzen, C.J., 1972. Yellow-green algae with chlorophyllide c. Journal of Phycology 8, 10–14.

Hansen, D.V., Rattray, M., 1966. New dimensions in estuary classification. Limnology and Oceanography 11, 319–326.

Harrison, P.J., Waters, R.E., Taylor, F.J.R., 1980. A broad spectrum artificial medium for coastal and open ocean phytoplankton. Journal of Phycology 16, 28–35.

Humborg, C., 1997. Primary productivity regime and nutrient removal in the Danube estuary. Estuarine, Coastal and Shelf Science 45, 579–589.

Humborg, C., Danielsson, A., Sjöberg, B., Green, M., 2003. Nutrient land-sea fluxes in oligotrophic and pristine estuaries of the Gulf of Bothnia, Baltic Sea. Estuarine, Coastal and Shelf Science 56, 781–793.

Ibanez, C., Saldana, J., Prat, N., 1999. A model to determine the advective circulation in a three layer, Salt Wedge Estuary: application to the Ebre River Estuary. Estuarine, Coastal and Shelf Science 48, 271–279.

Kay, D.J., Jay, D.A., 2003. Interfacial mixing in a highly stratified estuary – 1. Characteristics of mixing. Journal of Geophysical Research-Oceans 108. doi:10.1029/2000JC000252.

Lancelot, C., Mathot, S., 1987. Dynamics of a *Phaeocystis*-dominated spring bloom in Belgian coastal waters. 1. Phytoplankton activities and related parameters. Marine Ecology Progress Series 37, 239–248.

Legovic, T., Zutic, V., Vilicic, D., Grzetic, Z., 1996. Transport of silica in a stratified estuary. Marine Chemistry 53, 69–80.

Lionard, M., Muylaert, K., Van Gansbeke, D., Vyverman, W., 2005. Influence of changes in salinity and light intensity on growth of phytoplankton communities from the Schelde river and estuary (Belgium/The Netherlands). Hydrobiologia 540, 105–115.

Martin-Jézéquel, V., Hildebrand, M., Brzezinski, M.A., 2000. Silicon metabolism in diatoms: implications for growth. Journal of Phycology 36, 821–840.

Monsen, N.E., Cloern, J.E., Lucas, L.V., Monismith, S.G., 2002. A comment on the use of flushing time, residence time, and age as transport time scales. Limnology and Oceanography 47, 1545–1553.

Morris, A.W., Mantoura, R.F.C., Bale, A.J., Howland, R.J.M., 1978. Very low salinity regions of estuaries: important sites for chemical and biological reactions. Nature 274, 678–680.

Muylaert, K., Sabbe, K., 1999. Spring phytoplankton assemblages in and around the maximum turbidity zone of the estuaries of the Elbe (Germany), the Schelde (Belgium/The Netherlands) and the Gironde (France). Journal of Marine Systems 22, 133–149.

Officer, C.B., Ryther, J.H., 1980. The possible importance of silicon in marine eutrophication. Marine Ecology Progress Series 3, 83–91.

Orive, E., Iriarte, A., DeMadariaga, I., Revilla, M., 1998. Phytoplankton blooms in the Urdaibai estuary during summer: physico-chemical conditions and taxa involved. Oceanologica Acta 21, 293–305.

Paasche, E., 1980a. Silicon content of five marine plankton diatom species measured with a rapid filter method. Limnology and Oceanography 25, 474–480.

Paasche, E., 1980b. Silicon. In: Morris, I. (Ed.), The Physiological Ecology of Phytoplankton. Blackwell Scientific Publications, Oxford, pp. 259–284.

Patel, D., Guganesharajah, K., Thake, B., 2004. Modelling diatom growth in turbulent waters. Water Research 38, 2713–2725.

Pritchard, D.W., 1967. What is an estuary? Physical point of view. In: Lauff, G.H. (Ed.), Estuaries. American Association for the Advancement of Science, publication N° 83, Washington, pp. 3–5.

Ragueneau, O., Lancelot, C., Egorov, V., Vervlimmeren, J., Cociasu, A., Déliat, G., Krastev, A., Daoud, N., Rousseau, V., Popovitchev, V., Brion, N., Popa, L., Cauwet, G., 2002. Biogeochemical transformations of inorganic nutrients in the mixing zone between the Danube River and the North-western Black Sea. Estuarine, Coastal and Shelf Science 54, 321–336.

Rijstenbil, J.W., 1988. Selection of phytoplankton species in culture by gradual salinity increase. Netherlands Journal of Sea Research 22, 291–300.

Romero, J.R., Hipsey, M.R., Antenucci, J.P., Hamilton, D., 2003. Computational Aquatic Ecosystem Dynamics Model: CAEDYM. v2.0 Science Manual. Centre for Water Research. University of Western Australia.

Roubeix, V., 2007. Biogeochemical transformations and transfer of silicon in the river-sea transition zone: The role of planktonic diatoms. Ph.D. Thesis, Université Libre de Bruxelles, Belgium, 718 pp.

Sarthou, G., Timmermans, K.R., Blain, S., Tréguer, P., 2005. Growth physiology and fate of diatoms in the oceans: a review. Journal of Sea Research 53, 25–42.

Shafik, H.M., Herodek, S., Voros, L., Presing, M., Kiss, K.T., 1997. Growth of *Cyclotella meneghiniana* Kütz. I. Effects of temperature, light and low rate of nutrient supply. Annales de Limnologie 33, 139–147.

Sheldon, J.E., Alber, M., 2002. A comparison of residence time calculations using simple compartment models of the Altamaha River estuary, Georgia. Estuaries 25, 1304–1317.

Smayda, T.J., 1990. Novel and nuisance phytoplankton blooms in the sea: evidence for a global epidemic. In: Graneli, E., Sundström, B., Edler, L., Anderson, D.M. (Eds.), Toxic Marine Phytoplankton. Elsevier, Amsterdam, pp. 20–40.

Soetaert, K., Herman, P.M.J., Kromkamp, J., 1994. Living in the twilight: estimating net phytoplankton growth in the Westerschelde estuary (The Netherlands) by means of an ecosystem model (MOSES). Journal of Plankton Research 16, 1277–1301.

Sorokin, C., 1973. Dry weight, packed cell volume and optical density. In: Stein, J.R. (Ed.), Handbook of Physiological Methods: Culture Methods and Growth Measurements. Cambridge University Press, Cambridge, pp. 322–343.

Sullivan, B.E., Prahl, F.G., Small, L.F., Covert, P.A., 2001. Seasonality of phytoplankton production in the Columbia River: a natural or anthropogenic pattern? Geochimica et Cosmochimica Acta 65, 1125–1139.

Tilman, D., Kilham, S.S., 1976. Phosphate and silicate growth and uptake kinetics of the diatoms *Asterionella formosa* and *Cyclotella meneghiniana* in batch and semicontinuous culture. Journal of Phycology 12, 375–383.

Van Cappellen, P., Dixit, S., Gallinari, M., 2002. Biogenic silica dissolution and the marine Si cycle: kinetics, surface chemistry and preservation. Oceanis 28, 417–454.

Veldhuis, M.J.W., Admiraal, W., 1987. Influence of phosphate-depletion on the growth and colony formation of *Phaeocystis-Pouchetii*. Marine Biology 95, 47–54.

Yamada, S.S., D'Elia, C.F., 1984. Silicic acid regeneration from estuarine sediment cores. Marine Ecology Progress Series 18, 113–118.

Yin, K.D., Qian, P.Y., Chen, J.C., Hsieh, D.P.H., Harrison, P.J., 2000. Dynamics of nutrients and phytoplankton biomass in the Pearl River estuary and adjacent waters of Hong Kong during summer: preliminary evidence for phosphorus and silicon limitation. Marine Ecology Progress Series 194, 295–305.